Chemical and biological sensors

Electrochemical Investigation of TLR4/MD-2-Immobilized Polyaniline and Hollow Polyaniline Nanofibers: Toward Real-Time Triaging of Gram-Negative Bacteria Responsible for Delayed Wound Healing

Rahul Gangwar[1], Pravat Kumar Sahu[2], Karri Trinadha Rao[1], Patta Supraja[1,3], Suryasnata Tripathy[1,4], Challapalli Subrahmanyam[2], and Siva Rama Krishna Vanjari[1]

[1]*Department of Electrical Engineering, Indian Institute of Technology, Hyderabad 502284, India*
[2]*Department of Chemistry, Indian Institute of Technology, Hyderabad 502284, India*
[3]*Department of Electronics and Communication Engineering, SRM University AP, Amaravati 522240, India*
[4]*MESA+ Institute for Nanotechnology, University of Twente, 7500 AE Enschede, The Netherlands*

Manuscript received 10 September 2023; revised 10 October 2023; accepted 13 October 2023. Date of publication 19 October 2023; date of current version 17 November 2023.

Abstract—Detecting gram −ve bacterial colonies is crucial in addressing the clinical challenges associated with chronic wounds and delayed healing. These bacteria can exacerbate wound conditions, hindering natural healing and potentially leading to infections. The electrochemical sensing platform presented in this study serves as a valuable tool for healthcare professionals to make timely and targeted treatment decisions. Toward this, we developed a cost-effective electrochemical sensing platform leveraging the TLR4/MD-2 complex to detect gram −ve bacterial colonies. Our biosensors were meticulously fashioned using polyaniline (PANi) and hollow PANi (HPANi) nanofibers. Notably, the HPANi-based sensors, owing to their distinctive hollow structure, facilitated amplified responses under comparable experimental conditions compared with PANi-based counterparts. The designed sensing platform demonstrated exceptional accuracy in identifying *Escherichia coli* (gram −ve), showcasing a theoretical detection limit of 0.215 CFU/mL for PANi and a remarkably improved 0.14 CFU/mL for HPANi. These sensors displayed outstanding selectivity for gram −ve bacteria, even amidst gram +ve bacteria and fungi. Moreover, our platform demonstrated remarkable sensitivity, yielding 3.04 $((\Delta R/R)/CFU/mL)/cm^2$ for the HPANi-based sensor, surpassing the performance of the PANi-based sensor at 1.98 $((\Delta R/R)/CFU/mL)/cm^2$.

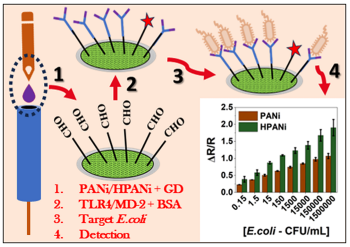

Index Terms—Chemical and biological sensors, electrochemical biosensor, gram-negative bacteria, hollow polyaniline (PANi) nanofibers, toll-like receptors.

I. INTRODUCTION

Wound healing in chronic wounds is significantly hampered by pathogenic bacteria. In order to provide an effective treatment and stop bacterial infection, these bacteria should be identified quickly and accurately. Culture-based approaches, commonly used in traditional bacterial identification procedures, take time and frequently call for specialized lab equipment. As a result, there is an urgent need for quick and accurate techniques that enable the real-time detection of bacteria [1], [2], [3]. Electrochemical biosensors have recently become prominent as promising platforms for detecting various microorganisms [4], [5], [6]. Among the various materials investigated for electrochemical biosensing, the conductive polymer polyaniline (PANi) has generated significant interest primarily due to its tunable electrical conductivity. Notably, its conducting properties result from the delocalized π-electrons within the polymer backbone. PANi also seems an ideal choice for such applications due to the ease of surface functionalization. Using well-known surface chemistry protocols, PANi nanofibers can be easily decorated with specific recognition components (such as antibodies, single-stranded nucleotides, and aptamers), facilitating selective capture and identification of specific target analytes [7], [8], [9], [10], [11]. In this context, hollow PANi (HPANi) nanostructures present additional benefits while maintaining the surface functionality offered by PANi. HPANi's open-ended hollow structure offers a higher surface-to-volume ratio, which, in turn, results in improved performance by lowering detection limits and enhancing sensitivity. Furthermore, unlike solid PANi nanofibers, which display both surface and bulk transport, the electrical transport in HPANi nanofibers is predominately surface-based, making them more responsive and susceptible to surface conditions [12]. Our group previously published reports on polypyrrole and PANi nanofiber-based immunosensors. These sensors were intended to detect disease-specific DNA hybridization events and antibody-antigen interactions [13], [14]. In this work, we evaluate the electrochemical performance of PANi and HPANi nanofibers toward the real-time identification of gram −ve bacteria. Herein, we have compared the performance of TLR4/MD-2 immobilized PANi and HPANi nanofibers while focusing on detecting entire gram −ve bacterial cells. TLR4, a member of the Toll-like receptor family combined with Myeloid differentiation factor-2 (MD-2) forms a heterodimer complex and recognizes explicitly the Lipopolysaccharides (LPS) layer on the gram −ve bacteria. TLRs can be used against various gram −ve or

Corresponding author: Siva Rama Krishna Vanjari (e-mail: svanjari@ee.iith.ac.in).
Associate Editor: Sanket Goel.
Digital Object Identifier 10.1109/LSENS.2023.3326108

TABLE 1. Comparison of LDR and LoDs With Existing Literature on TLR-4-Based Detection

Target	LDR	LoD	Ref.
LPS	1 – 2,000 ng/ml	3 ng/ml	[16]
Lysed cells	1 - 10^5 cells/mL	1 cell/mL	[17]
LPS	1 – 10,000 ng/mL	100 cells/mL	[15]
Endotoxins	0.0005 - 5 EU/mL	0.0002 EU/mL	[18]
E.coli (LPS)	***1.5×10^{-1} – 1.5×10^{6} CFU/mL***	***0.14 CFU/mL for HPANi biosensor***	***This work***

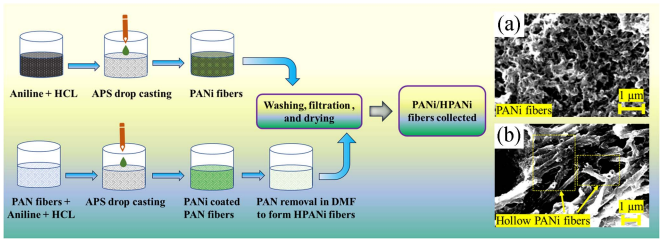

Fig. 1. Synthesis and characterization of PANi and HPANi nanofibers (inset showing the SEM images of PANi and HPANi nanofibers).

gram +ve bacterial species, unlike antibodies unique to one type of bacterium. High sensitivity and specificity, quick response times, and label-free detection are only a few benefits of TLR4-based detection [4], [15]. In recent years, bacterial detection has been widely reported using TLR4 to recognize gram −ve bacterial LPS. A comparative analysis of the proposed sensing platform with some of the previously published literature is presented in Table 1.

II. METHODS AND PROTOCOLS

A. PANi and HPANi Nanofiber Synthesis and Characterization

A previously established technique was employed to produce PANi nanofibers using wet chemical synthesis [7]. Briefly, a mixture of 0.05 M aniline and 0.05 M ammonium peroxydisulphate (in 1 M HCl) was stirred for 2 h to produce a dark green precipitate. It was washed several times with deionized water to remove the acidic residue and filtered thereafter to obtain the required PANi nanofibers. These nanofibers were then dried in a hot air oven (at 80 °C for 12 h) and finally collected in the powdered form. To obtain the HPANi nanofibers, first, an electrospun polyacrylonitrile (PAN) nanofiber mat was synthesized, which was later coated with PANi by in-situ chemical polymerization technique. Subsequently, the PANi-coated PAN nanofiber mats were stirred in dimethylformamide, which dissolved the PAN sacrificial layer. The HPANi nanofibers were finally obtained by filtering and drying the remaining precipitate for 12 h at 80 °C. The morphological analysis of PANi and HPANi fibers was conducted using scanning electron microscopy (SEM). In the inset of Fig. 1, the SEM images of PANi (Fig. 1(a)) and HPANi (Fig. 1(b)) nanofibers are presented. These images reveal distinct characteristics: the hollow PANi fibers exhibit an approximate diameter of 400 nm, notably larger than the PANi fibers, which measure around 50 nm. Both types of fibers display an extended cylindrical feature spanning several micrometers. The increase in diameter observed in the hollow PANi fibers can be attributed to their growth atop PAN fibers and can be visualized in the inset of Fig. 1. The inset serves as a confirmation of the successful

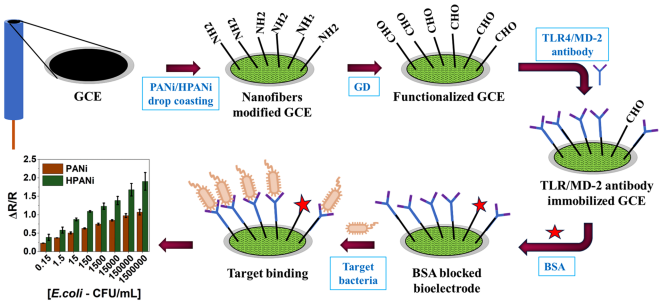

Fig. 2. Various steps demonstrating the preparation of bioelectrode (inset graph depicting the normalized response comparison of PANi and HPANi modified biosensor).

synthesis of hollow PANi fibers. It reveals that the vertically oriented HPANi fibers exhibit an open and hollow structure, in contrast with the uniform thickness of the pure PANi fibers.

B. Bacterial Sample Preparation

The bacterial samples were prepared following the established protocol detailed in our earlier publication [4], [5], [6]. Summarizing, we used brain heart infusion broth for the cultivation of *Escherichia coli (E.coli), Pseudomonas aeruginosa (P.aeruginosa), Enterococcus faecalis (E.faecalis), Staphylococcus aureus (S.aureus), and Candida albicans (C.albicans) (fungi).* These cultures were incubated at 37 °C until they reached an optical density of 0.1, equivalent to approximately 1.5×10^8 CFU/mL. To facilitate the testing of various concentrations of bacteria and fungi, we performed serial dilutions in phosphate-buffered saline (PBS) as follows: 1.5×10^{-1}, 1.5×10^{0}, 1.5×10^{1}, 1.5×10^{2}, 1.5×10^{3}, 1.5×10^{4}, 1.5×10^{5}, and 1.5×10^{6} CFU/mL. Prior to the serial dilution process, all prepared samples were thoroughly vortexed to achieve a homogeneous solution.

C. Electrochemical Biosensor Preparation

As shown in Fig. 2, we initiated the immunosensor preparation by drop-casting an optimized volume of 3 µL of PANi and HPANi nanofiber solution (5 mg/mL in ethanol) onto pristine glassy carbon (GCE) electrodes. Subsequently, we subjected them to hot air drying at 37 °C for 30 min. This ensured complete solvent evaporation, leaving the nanofibers securely adhered to the electrodes. It is important to note that we avoided subjecting PANi to high-heat treatment due to its temperature sensitivity. The surface modification of both PANi and hollow PANi nanofibers was carried out by immersing the nanofiber-coated GCEs in a 2.5% glutaraldehyde solution at 4 °C for 6 h [7]. Later, the TLR4/MD-2 complex (5 µg/ml) was covalently bound to the nanofibers through imide chemistry. We then used bovine serum albumin to block any unoccupied active sites on the nanofibers, preventing nonspecific binding of the target analyte. Following these procedures, the bioelectrodes were thoroughly cleaned with PBS, left to air-dry at room temperature, and subsequently stored in a refrigerator at 4 °C in airtight containers for future use.

III. RESULTS AND DISCUSSION

A. Electrochemical Characterization of PANi/HPANi Nanofibers

All electrochemical measurements were conducted in a 5 mM ferro-ferri $(Fe(CN)_6)^{3-/4-}$ redox couple solution prepared in 0.1 M

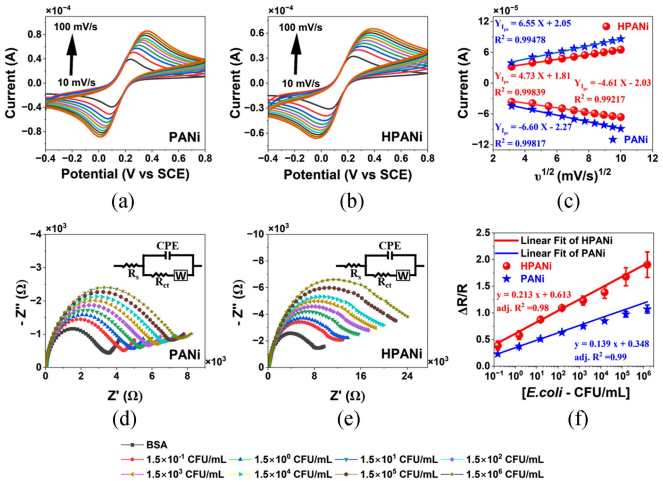

Fig. 3. CV of (a) PANi and (b) HPANi nanofibers drop casted GCE at various scan rates (10–100 mV). (c) Linear fitting curve of peak anodic and cathodic currents w.r.t. square-root of various scan rates. Detection of *E.coli* using EIS with (d) PANi and (e) HPANi modified bioelectrode. (f) Calibration curve obtained for *E.coli* detection using PANi and HPANi drop casted bioelectrodes (N = 3).

PBS, using GCE working electrodes, platinum wire counter electrode, and saturated calomel reference electrode. As depicted in Fig. 3(a) and (b), we initially assessed the suitability of PANi and HPANi-modified GCEs for electrochemical sensing using cyclic voltammetry (CV) within the voltage range of −0.4 to +0.8 V. The resulting CV exhibited slight variations in peak potential, with the anodic (I_{pa}) and cathodic (I_{pc}) peak currents increasing with scan rate (υ). This behavior suggested the quasi-reversible nature of the fabricated working electrode, further supported by Fig. 3(c), where the anodic and cathodic peak currents exhibited linear relationships with the square root of the scan rate, demonstrating an accuracy of 99% with $I_{pa}/I_{pc} \approx 1$. Furthermore, Fig. 3(c) revealed that the current recorded for PANi drop-casted GCEs was notably higher than that for HPANi drop-casted GCEs. This can be attributed to the distinct transport mechanisms: the current observed in PANi drop-casted GCEs primarily arises from bulk transport, while HPANi drop-casted GCEs rely predominantly on surface transport. Additionally, the smaller diameter of PANi fibers (∼50 nm) in comparison to HPANi nanofibers (∼400 nm) results in a higher aspect ratio and greater surface area, translating to a larger current in the case of PANi drop-casted nanofibers. As elaborated in the following section, this increased current for PANi nanofibers directly correlates with lower resolution and sensitivity in the context of bacterial detection.

B. Electrochemical Detection of Gram −ve Bacteria

Fig. 3(d) and (e) illustrate the Nyquist plots, covering a frequency range from 0.1 Hz to 0.1 MHz, obtained from electrochemical impedance spectroscopy (EIS) conducted on PANi and HPANi-modified bioelectrodes. These plots were generated before and after binding various target *E.coli* concentrations ranging from 1.5×10^{-1} to 1.5×10^{6} CFU/mL. To ensure data reliability, a minimum of three electrodes were used to record the response to each target dose. Herein, an incubation period of 30 min (attributing to an overall testing time of 40±5 min) was used for target binding onto the immobilized TLR4/MD-2 receptors. Notably, the diameter of the semicircle illustrated in the Nyquist plots represents the charge transfer resistance (R_{ct}), and as illustrated in Fig. 3(d) and (e), there is a noticeable increase in R_{ct} with each successive increment in target *E.coli* concentration. This indicates a degradation in reaction kinetics at the bioelectrode/electrolyte interface with increasing analyte concentration, which can be explained as follows. Upon binding with the TLR4/MD-2 protein heterodimer, the negatively charged LPS layer present in gram −ve bacteria like *E.coli* impedes the flow of the negatively charged redox couple to the electrode/electrolyte interface. Consequently, an electrostatic barrier is formed, leading to a reduction in the electrochemical kinetics of the biosensor and an increase in R_{ct}. As the bacterial population increases, more LPS molecules bind to the sensor's surface, which further increases the R_{ct}. The electrical behavior of the sensing mechanism was assessed using a modified Randle's circuit, as depicted in the inset of Fig. 3(d) and (e). Experimental values for the circuit elements were derived by fitting the impedance data obtained from the experiments. Within this circuit, the parameters R_s, R_{ct}, W, and CPE represent the solution resistance, charge transfer resistance, Warburg impedance, and the constant phase element, respectively. The constant phase element characterizes the behavior of a double-layer capacitance. Fig. 3(f) illustrates the calibration curve, where the normalized change in R_{ct} ($\Delta R/R$) is plotted against different concentrations of target *E.coli*. $\Delta R/R$ was computed as $(R_{ctn}–R_{ct0})/R_{ct0}$, with R_{ct0} representing the charge transfer resistance of the bioelectrode without the target and R_{ctn} (n = −1–6) representing the values obtained at various concentrations of target *E.coli*. Each data point on the graph is associated with error bars that signify the standard deviation calculated from the data collected from at least three electrodes. A linear regression model was employed to model the relationship depicted in Fig. 3(f), yielding a linear equation with an adjusted R-square value of 0.98 and 0.99 for HPANi and PANi-modified bioelectrodes, respectively. This high R-square value indicates the model's strong correlation and accuracy in predicting the bioelectrodes' behavior in response to varying concentrations of *E.coli*. Notably, the HPANi-based electrochemical sensor exhibited a higher normalized response than the PANi-based sensor. This enhanced response in the HPANi-based sensors can be attributed to their hollow morphology, which renders electronic transport more responsive to surface conditions when compared with solid PANi nanofibers. In the case of PANi, the contribution from bulk transport remains less influenced by changes in surface conditions, resulting in inferior responses. This directly translates to higher resolution for HPANi-based sensors, as evident in Fig. 3(f).

The proposed sensing platform demonstrated a sensitivity (defined as the slope of the calibration curves, normalized over the sensor's surface area) of 3.04 $((\Delta R/R)/CFU/mL)/cm^2$ for the HPANi-based sensor, surpassing the performance of the PANi-based sensor at 1.98 $((\Delta R/R)/CFU/mL)/cm^2$. The platform exhibited the capability to detect *E.coli* within a wide linear detection range (LDR) spanning from 1×10^{-1} to 1×10^{6} CFU/mL, achieving a limit of detection (LoD) of 0.215 CFU/mL for PANi and a significantly improved 0.14 CFU/mL for the HPANi-modified sensor. The theoretical LoD and sensitivity of the proposed biosensor were calculated using the formulas 3.3σ/slope and slope/area, respectively, with the slope derived from the linear fit of the calibration graph and σ representing the standard deviation of the blank response. Notably, the achieved LoD with the proposed sensing platform was remarkably low, with a wide LDR compared with prior literature (Table 1).

C. Reproducibility, Selectivity, and Interference

Since the analytical performance of the HPANi-based sensor was superior to the PANi-based sensor, we performed the reproducibility, selectivity, and interference studies with HPANi-modified bioelectrode.

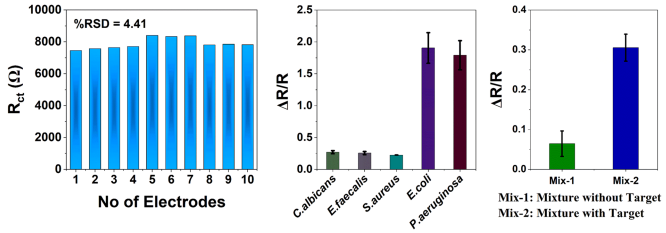

(a) (b) (c)

Fig. 4. (a) Reproducibility of the prepared HPANi-bioelectrodes. (b) Selectivity. (c) Interference of the HPANi-based biosensor.

As depicted in Fig. 4(a), these electrodes accounted for excellent reproducibility with a %RSD (relative standard deviation) of merely 4.41%. In addition, we performed interference and selectivity studies for point-of-care applications. These studies involved comparing the normalized response of the HPANi-modified bioelectrodes at high concentrations [1.5×10^6 CFU/mL] of nonspecific microorganisms, namely *S.aureus, E.faecalis, C.albicans*, and a mixture of these species, with the response obtained against *E.coli*. The mixture (Mix-1) comprised all three bacteria in equal ratios at concentrations mentioned above [1.5×10^6 CFU/mL]. The results, presented in Fig. 4(b), clearly show that the normalized change in R_{ct} was significantly higher for the target *E.coli* than the nonspecific targets, indicating excellent specificity of the proposed platform. Furthermore, as shown in Fig. 4(c), the immunosensor's response to the mixture of the nonspecific microorganisms [Mix-1 – 1.5×10^6 CFU/mL] was insignificant, with respect to the response obtained against the same mixture (Mix-1) containing *E.coli* [1.5×10^{-1} CFU/mL]. These findings underscore the platform's ability to distinguish target bacteria effectively from interfering species. To further showcase the versatility of the proposed platform in detecting gram −ve bacteria, a study involving another gram −ve bacterial strain, *P.aeruginosa*, was conducted. The sensor's response to *P.aeruginosa*, as appended in Fig. 4(b), was comparable to the response obtained for *E.coli* under identical experimental conditions. This is a testament to the fact that the proposed platform can swiftly identify the colonies of gram −ve bacteria. In the future, we plan to extend this work for real-time samples on Lab on a Chip portable devices.

IV. CONCLUSION

In this letter, our electrochemical sensing platform offers a cost-effective solution for the real-time detection of gram −ve bacteria, addressing the critical challenge of managing chronic wounds. The findings hold significant clinical potential for expedited wound healing and broader healthcare applications.

ACKNOWLEDGMENT

This work was supported by the Department of Science and Technology under Grant DST/NM/ NT/2021/01-1C. The authors would like to thank Ms. Sajmina Khatun and Dr. Aravind Kumar Rengan from the Department of Biomedical Engineering, IIT Hyderabad for providing us with the bacterial samples.

REFERENCES

[1] A. Omar, J. Wright, G. Schultz, R. Burrell, and P. Nadworny, "Microbial biofilms and chronic wounds," *Microorganisms*, vol. 5, no. 1, 2017, Art. no. 9, doi: 10.3390/microorganisms5010009.

[2] R. A. Cooper, T. Bjarnsholt, and M. Alhede, "Biofilms in wounds: A review of present knowledge," *J. Wound Care*, vol. 23, no. 11, pp. 570–582, 2014, doi: 10.12968/jowc.2014.23.11.570.

[3] K. Izadi and P. Ganchi, "Chronic wounds," *Clin. Plast. Surg.*, vol. 32, no. 2, pp. 209–222, 2005, doi: 10.1016/j.cps.2004.11.011.

[4] R. Gangwar, D. Ray, S. Khatun, C. Subrahmanyam, A. K. Rengan, and S. R. K. Vanjari, "Toll-like receptor-immobilized carbon paste electrodes with plasma functionalized amine termination: Towards real-time electrochemical based triaging of gram-negative bacteria," *Biosensors Bioelectron.*, vol. 241, 2023, Art. no. 115674, doi: https://doi.org/10.1016/j.bios.2023.115674.

[5] R. Gangwar et al., "Plasma functionalized carbon interfaces for biosensor application: Toward the real-time detection of Escherichia coli O157: H7," *ACS Omega*, vol. 7, no. 24, pp. 21025–21034, 2022, doi: 10.1021/acsomega.2c01802.

[6] R. Gangwar, K. T. Rao, S. Khatun, A. K. Rengan, C. Subrahmanyam, and S. R. Krishna Vanjari, "Label-free miniaturized electrochemical nanobiosensor triaging platform for swift identification of the bacterial type," *Analytica Chimica Acta*, vol. 1233, 2022, Art. no. 340482, doi: 10.1016/j.aca.2022.340482.

[7] S. Tripathy, R. Gangwar, S. R. K. Vanjari, and S. G. Singh, "Polyaniline nanofibers as chemiresistive transducers: Seeded synthesis, characterization and DNA sensing," in *Proc. IEEE 5th Int. Conf. Emerg. Electron.*, 2020, pp. 1–4.

[8] A. Mulchandani and N. V. Myung, "Conducting polymer nanowires-based label-free biosensors," *Curr. Opin. Biotechnol.*, vol. 22, no. 4, pp. 502–508, 2011.

[9] I.-A. Pavel, S. Lakard, and B. Lakard, "Flexible sensors based on conductive polymers," *Chemosensors*, vol. 10, no. 3, 2022, Art. no. 97.

[10] S. A. Ansari, N. Parveen, T. H. Han, M. O. Ansari, and M. H. Cho, "Fibrous polyaniline@manganese oxide nanocomposites as supercapacitor electrode materials and cathode catalysts for improved power production in microbial fuel cells," *Phys. Chem. Chem. Phys.*, vol. 18, no. 13, pp. 9053–9060, 2016, doi: 10.1039/c6cp00159a.

[11] N. Parveen, N. Mahato, M. O. Ansari, and M. H. Cho, "Enhanced electrochemical behavior and hydrophobicity of crystalline polyaniline@graphene nanocomposite synthesized at elevated temperature," *Composites Part B: Eng.*, vol. 87, pp. 281–290, 2016, doi: 10.1016/j.compositesb.2015.10.029.

[12] A. M. Seif, F. Ahmadi Tabar, A. Nikfarjam, F. Sharif, H. Hajghassem, and S. Mazinani, "Hollow polyaniline nanofibers for highly sensitive ammonia detection applications," *IEEE Sens. J.*, vol. 19, no. 21, pp. 9616–9623, Nov. 2019, doi: 10.1109/JSEN.2019.2927732.

[13] P. Supraja, S. Tripathy, and S. G. Singh, "Smartphone-powered, ultrasensitive, and selective, portable and stable multi-analyte chemiresistive immunosensing platform with PPY/COOH-MWCNT as bioelectrical transducer: Towards point-of-care TBI diagnosis," *Bioelectrochemistry*, vol. 151, 2023, Art. no. 108391.

[14] P. Supraja, S. Tripathy, S. R. Krishna Vanjari, and S. G. Singh, "Label-free, ultrasensitive and rapid detection of FDA-approved TBI specific UCHL1 biomarker in plasma using MWCNT-PPY nanocomposite as bio-electrical transducer: A step closer to point-of-care diagnosis of TBI," *Biosensors Bioelectron.*, vol. 216, 2022, Art. no. 114631, doi: 10.1016/j.bios.2022.114631.

[15] R. M. Mayall, M. Renaud-Young, N. W. C. Chan, and V. I. Birss, "An electrochemical lipopolysaccharide sensor based on an immobilized toll-like receptor-4," *Biosensors Bioelectron.*, vol. 87, pp. 794–801, 2017, doi: 10.1016/j.bios.2016.09.009.

[16] D. Lin, K. D. Harris, N. W. C. Chan, and A. B. Jemere, "Nanostructured indium tin oxide electrodes immobilized with toll-like receptor proteins for label-free electrochemical detection of pathogen markers," *Sensors Actuators B: Chem.*, vol. 257, pp. 324–330, 2018, doi: 10.1016/j.snb.2017.10.140.

[17] R. M. Mayall, M. Renaud-Young, E. Gawron, S. Luong, S. Creager, and V. I. Birss, "Enhanced signal amplification in a toll-like receptor-4 biosensor utilizing ferrocene-terminated mixed monolayers," *ACS Sensors*, vol. 4, no. 1, pp. 143–151, 2019, doi: 10.1021/acssensors.8b01069.

[18] T. Y. Yeo et al., "Electrochemical endotoxin sensors based on TLR4/MD-2 complexes immobilized on gold electrodes," *Biosensors Bioelectron.*, vol. 28, no. 1, pp. 139–145, 2011, doi: 10.1016/j.bios.2011.07.010.